ETH
Eidgenössische Technische Hochschule Zürich
Swiss Federal Institute of Technology Zurich

Department of Physics
Laboratory for Solid State Physics
Quantum Device Lab

Semester Thesis

Temperature Stabilization of a Cu-Sample-Holder on the 4 K-Stage of a Pulse Tube Cooler

Matthias Mergenthaler
September 2012

Supervisors
Dr. Klaus Reim
Tobias Thiele

Principle Investigator
Prof. Dr. Andreas Wallraff

Abstract

For this semester thesis different techniques for the temperature stabilization of a Cu-sample-holder on the 4 K-stage of a pulse tube cooler were studied. The best temperature stabilization technique, reducing the temperature fluctuations from 200 mK to about 8 mK (at 6.1 K), is implemented with a LabView program.

Contents

1 Introduction

For my semester thesis I joined the Quantum Device Lab[1] at ETH Zurich and assisted Dr. Klaus Reim and Tobias Thiele with the *"Hybrid Cavity Quantum Electrodynamics with Atoms and Circuits"*[2] project.

1.1 Hybrid Quantum System

In the last decades research in the field of quantum information science has been mainly focusing on the implementation of microscopic quantum systems, such as atoms or ions, or solid state systems. The conceptual ideas behind the two different systems are very similar but have not been joined together in a single system yet. The hybrid quantum system plans to combine the strengths of both systems by coupling them coherently.

In this particular experiment, Rydberg atoms are coupled to photons generated by a one-dimensional coplanar microwave resonator or a microwave resonating cavity. In comparison to quantum dots or superconducting qubits, Rydberg atoms have long coherence times (up to 70 ms, for $n = 60$) and would serve as a storage for quantum information extracted from Circuit Quantum Electrodynamics. In the future, the hybrid system in question would be used as a RAM in a quantum computer. In Figure 1 the schematics of the hybrid quantum system is shown [1].

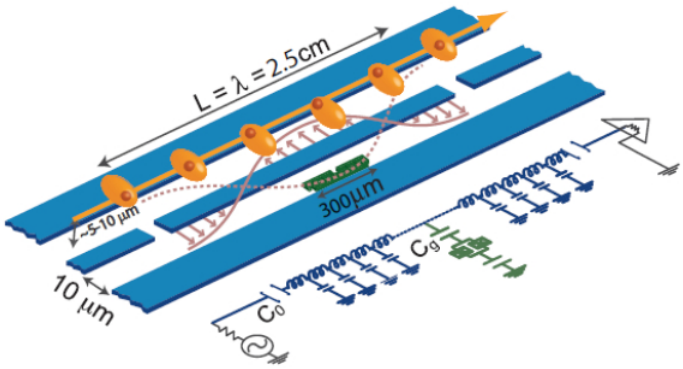

Figure 1: Schematics of a circuit coplanar microwave resonator (blue) with an integrated superconducting qubit (green) and Rydberg atoms (orange) from a beam passing across the chip [1].

1.2 Rydberg Atoms

Rydberg atoms are atoms with its outer-shell electron being excited (to $n \gtrsim 15$), such that it is located far away from the nucleus. They can have large electric dipole moments ($\sim 1500\, e\, a_0$, $n = 60$) that scale as $\vec{d} \propto n^2$. Neighboring Rydberg states have an energy difference that scales with n^{-3} and the corresponding transition frequencies lie in the millimeter and microwave range[3]. The excited state life time

[1] QUDEV, www.qudev.ethz.ch
[2] HYBRIDQED
[3] for $n>25$

of Rydberg atoms scales as n^3 for low l-states and up to n^5 for high l-states. This results in a lifetime of 70 ms for circular $n = 60$ for example.

These properties of Rydberg atoms make them especially suitable for coupling to microwave photons.

1.3 Microwave Resonator

The microwave resonator is a coplanar quasi-one-dimensional waveguide. The waveguide consists of a center-conductor which is separated by gaps from two metallic ground planes. The structure is etched into a superconducting layer (NbTiN) on a dielectric substrate (sapphire) and guides microwaves in the gaps.

The resonator has a characteristic resonance frequency ν_0 and the resonance is lorentzian shaped. The quality factor[4] of such a resonator is described by the quotient of its resonance frequency ν_0 and the full width at half maximum $\delta\nu$ [2]:

$$\nu_0 = \frac{1}{2\pi\sqrt{L_0 C}} \tag{1}$$

$$Q = \frac{\nu_0}{\delta\nu} \tag{2}$$

Measurements in [2] showed that the transmission of the resonators as well as the Q-factors depend on temperature. Throughout the analysis temperature oscillations around a fixed value were observed. The temperature oscillations have an overall amplitude of about 200 mK with a distinct frequency of 1.41178 Hz[5]. Those rather large temperature oscillations influence the frequency of the resonator, since its kinetic inductance is very temperature dependent.

In order to get a stable resonance, in order to drive transitions of Rydberg atoms, the temperature of the resonator's sample-holder needs to be stabilized. This is the purpose of the following semester-thesis.

2 Theory

There are two ways to reduce large temperature fluctuations in a pulse tube cooler. One of them is to thermally decouple the sample from its cold head. Thus the system is more inert and does not follow the "fast" (1.41178 Hz)[6] temperature fluctuations. The second option is to control the temperature of the sample with an active heating source. In this thesis a combination of both techniques is used.

2.1 Fiber Reinforced Plastic Damping

Partially decoupling the sample from the cold head is done with a material that does not conduct heat very well, such that the temperature of the sample-holder (SH) can not follow the temperature oscillations. Reducing the heat transfer from the base plate onto the SH also results in a higher temperature than the actual temperature of the cold head. A good material that does not conduct heat too well but also does

[4] Q-factor
[5] See chapter 4.2.
[6] See chapter 4.2.

not raise the temperature of the SH too much, is fiber reinforced plastic (FRP) as suggested by [3, 4]. They present a model and an experiment, reducing the effect of temperature fluctuations of the pulse tube cooler from 200 mK to about 0.7 mK but at a base temperature of 4.2 K. A similar procedure was applied to our experimental setup[7].

In both papers, Nakamura & Hasegawa placed FRP between the cold head and the sample stage, to reduce the heat transfer. D. Nakamura[3] suggests a one-dimensional heat transfer model that calculates the attenuation ratio AR (3) of the temperature fluctuation with frequency f, for a given FRP with thickness x and thermal diffusivity α.

$$\mathrm{AR} = \frac{\tilde{T}_1}{\tilde{T}_0} = exp\left(-\sqrt{\frac{\pi f}{\alpha}}x\right) \tag{3}$$

In this model $\tilde{T}$ corresponds to the peak-to-peak value of the temperature fluctuation. D. Nakamura suggests that the thermal diffusivity α of the FRP should be between 10^{-4} and $10^{-7}\frac{m^2}{s}$ to get a reasonable attenuation ratio.

To reduce the temperature fluctuations mentioned in chapter 1.3 we placed an FRP damper between the 4 K stage of the pulsed tube cooler and the sample-holder[8]. The FRP damper, with thickness $x = 0.8\,mm$ reduced the peak-to-peak value of the temperature fluctuations from 200 mK to 68 mK. Using the model introduced by D. Nakamura, this corresponds to a thermal diffusivity of

$$\alpha = 2.4724 \times 10^{-6}\,\frac{m^2}{s},$$

using a frequency of $f = 1.41178$ Hz for the temperature fluctuation and an attenuation ratio AR of 0.34.

2.2 Thermal Heat Transfer

The heat flow through the FRP, with density $\rho = 1779.9928\,\frac{kg}{m^3}$, specific heat capacity $c_p = 960 - 1300\,\frac{J}{kg\,K}$ [5] and thermal conductivity

$$k = \alpha \cdot \rho \cdot c_p = 4.22489 - 5.7212\,\frac{W}{m\,K}$$

is calculated with Fourier's law (4).

$$\frac{\partial Q}{\partial t} = -k \oint_S \vec{\nabla} T \cdot d\vec{A} \tag{4}$$

With a Temperature gradient of $\vec{\nabla} T = 0.77$ K (at a base temperature of 5.305 K[9]) this equates to a thermal heat flow of $\frac{\partial Q}{\partial t} = P_{FRP} = 0.62 - 0.85$ mW through the FRP damper. The final temperature of the sample holder is higher than the 4 K stage, since heat is radiated from the 40 K shield onto the sample-holder. This must be in the range of the calculated heat flow through the damper.

[7] See Chapter 3.

[8] For details see chapter 3.3.

[9] Increased base temperature due to problems with the pulse tube cooler. For further details see chapter 3.1.

Idealizing the 40 K shield as a black body, the Stefan-Boltzmann law (Eqn. 5) is applicable to this setting.

$$P = \sigma T^4 A \tag{5}$$

Using this law and a surface area of the 40 K shield of $A = 0.172884$ m^2 the radiated heat is $P_{40K} = 25.0945$ mW. Not all of the radiated heat is incident on the sample-holder, therefore we need to correct the radiated heat by a geometrical factor. This factor is equal to the ratio of the surfaces of the 40 K shield and the sample-holder

$$r = \frac{A_{SH}}{A_{40\,K}} = \frac{0.054\,m^2}{A_{40\,K}} = 0.0312348.$$

The result for the incident radiation is equal to

$$P_{inc} = r \cdot P_{40\,K} = 0.78\,mW$$

and corresponds really well to the heat transferred through the FRP damper.

2.3 Ziegler-Nichols Method

During the course of the thesis, an active temperature control with a PID controller was tried. In order to tune the PID Controller of the LakeShore 340 temperature controller, the very common Ziegler-Nichols Method [6] was used. To find the ideal settings for the P, I and D gains, the I and D are first set to zero. The P gain, also called K_P, is then increased from zero to the ultimate gain K_U. The ultimate gain is the setting for P, at which the temperature signal oscillates with a constant amplitude. The period T_U of this oscillation and K_U are the used to find the correct values for the P, I and D gain. Table 1 shows the equations which are used to calculate the correct gain values [6].

Control Type	K_P	K_I	K_D
P	$K_U/2$		
P I	$K_U/2.2$	$1.2K_P/T_U$	
P I D	$0.6K_U$	$2K_P/T_U$	$K_PT_U/8$
some overshoot	$0.33K_U$	$2K_P/T_U$	$K_PT_U/3$
no overshoot	$0.2K_U$	$2K_P/T_U$	$K_PT_U/3$

Table 1: Ziegler-Nichols method, equations for control gains.

3 Experimental Setup

The experiment is done in a high vacuum chamber, and cooled with a pulse tube cooler to a temperature of 2.8 K[10]. The Rydberg atoms are being excited with a Nd:YAG-Laser, that is transmitted through the vacuum chamber. The current overall setup of the experiment is similar to the one described in [2, 7, 8]. Figure 2 shows the setup.

[10] 5 K in this thesis. For further details refer to chapter 3.1.

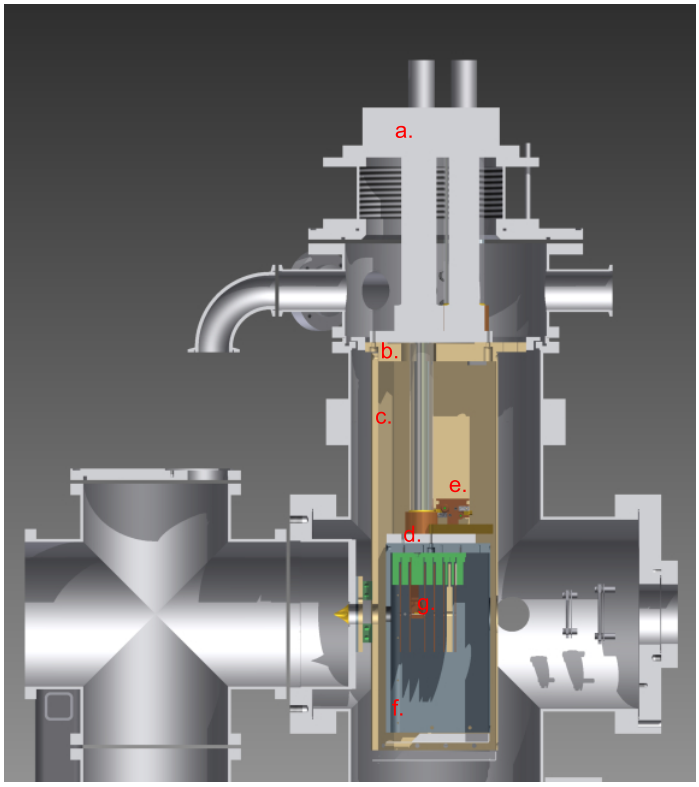

Figure 2: Experimental setup of the vacuum chamber: a. Pulse tube cooler, b. 40 K-stage, c. 40 K-shield, d. 4 K-stage, e. upper sample-holder, f. 4 K-shield, g. lower sample-holder.

3.1 Pulse Tube Cooler & Thermal Shields

In order to reach the low temperatures needed for the experiment a pulse tube cooler is used. The specific model is the *Cryomech PT415 Remote pulse tube refrigeration system* in connection with the *Cryomech CP1000 helium compressor*. The pulse tube cooler has two different cooling stages with a temperature of $40\,K$ and $4\,K$. The two cooling stages are separated by two thermalized copper shields. The cooling power of the pulse tube cooler is strong enough to cool the system down to $2.8\,K$ and $32\,K$ on each stage respectively. A cool-down from room-temperature to equilibrium takes about $2.5\,h$.

A pulse tube cooler works in a simple pattern. It exchanges heat by compressing and decompressing helium within the pulse tube. The basic structure of a pulse tube cooler consists of a compressor, a regenerator, a warm and a cold heat exchange as well as a pulse tube and a reservoir, as shown in Figure 3. The cooling cycle can be described in the following 4 steps:

1. The compressor compresses the helium in the pulse tube. Due to the compression the helium increases its temperature.

2. Since the helium is at higher pressure than the helium in the reservoir there is a helium flow from the pulse tube into the reservoir. The flow stops as soon as the pressure in the pulse tube is in equilibrium with the pressure in the

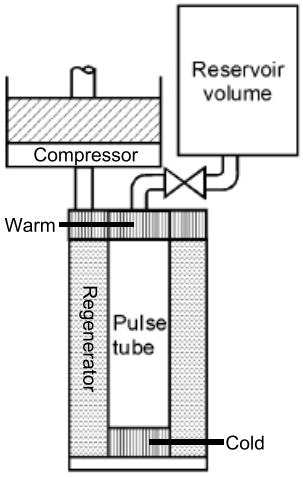

Figure 3: Pulse tube cooler schematic [9].

reservoir. Throughout this process heat is exchanged with the environment through the heat exchanger at the warm end of the pulse tube.

3. The compressor expands the helium adiabatically in the pulse tube and therefore cools it.

4. The cold, low-pressure helium is forced towards the cold end of the pulse tube by the pressure of the helium flow coming from the reservoir. By flowing through the heat exchanger at the cold end of the pulse tube, the helium picks up heat from the object being cooled. The flow stops when the pulse tube is in pressure equilibrium with the reservoir. Now the process repeats itself.

The crucial function of the pulse tube is the insulation of the process at its two ends. This means it needs to be long enough, such that gas from the warm end does not reach the cold end and vice versa, before the process is reversed. Therefore the helium in the middle of the pulse tube never leaves the pulse tube and forms an insulating temperature gradient. With the needle valve, shown in Figure 3, the phase between heat exchange and real helium flow can be adjusted.

Throughout the course of this thesis we encountered some problems with the pulse tube cooler, which lead to higher temperatures of the cold head and the sample stages. Our assumptions for the higher temperature where in the first place, that either some wires or other parts of the experimental setup were touching the 40 K-shield or that gas froze onto the thermal shields and the cold head. After thoroughly checking for those perturbations of the cooling mechanism, it was found not to be the reason. Further we could rule out "dirt" (N_2, O_2) in the He-line by pumping out a) the whole system and b) the cold head and refilling He. Therefore we were forced to conduct the experiment with higher base temperature ($\sim$5 K). Since none of our attempts helped, we assume that there is a major problem with the cold head; and did therefore sent the pulse tube back for a check to the manufacturer in the end.

3.2 Temperature Sensing System

For the temperature measurements the temperature controller *LakeShore Model 340* including the *LakeShore Model 3468 Eight-Channel Input Option Card* [10] is being used. The temperature sensing is done by 4 silicon diode sensors of the model *LakeShore DT-670C-CU* [10]. The sensors are placed on the $4\,K$-stage, on the $40\,K$-stage and shield and one on the upper sample holder. The 5th temperature sensor is placed on a second (lower) sample holder, enclosed in the $4\,K$-shield, which is not used nor mentioned in this thesis.

The LakeShore Model 340 can also control the temperature with an integrated proportional-integral-derivative PID controller, if a heater is connected to the Heater Output of one of the two control loops. The parameters P (proportional), I (integral) and D (derivative), Equation (6), can be auto tuned to achieve a certain setpoint temperature or be manually adjusted.

$$P_{Heater} = P\left(e + I\int e\cdot dt + D\frac{de}{dt}\right) \tag{6}$$

In (6) the variable $e = T_s - T_c$ is the current error between the setpoint temperature T_s and the current temperature T_c. The temperature controller has two integrated feedback loops that steer the two heater outputs. Feedback loop 1 has a maximum heater output power of $10\,W$ and feedback loop 2 a maximum power of $1\,W$. The LakeShore 340 temperature controller includes the extension card, and therefore can measure temperatures of up to 10 different temperature sensors. This has the disadvantage, that the more temperature sensors are connected, the slower is the read out rate. Furthermore the LakeShore 340 is able to tunnel the input signal of one temperature sensor onto one of its analog output channels. Those analog output channels convert the temperature into a voltage signal, whose scaling can be set arbitrarily.

3.3 Sample-Holder & Heater

As seen in Figure 2 the sample-holder, made out of OFHC copper is mounted on top of the $4\,K$-stage. Between the sample-holder and the $4\,K$-stage an FRP platelet with thickness $x = 0.8\,mm$ was placed and the sample-holder is screwed onto the stage with a stainless steel screw.

The space for the heating wire in Figure 4 is filled with a silk-isolated constantan wire, of resistance $R_1 = 52\,\Omega$. The constantan wire is connected with copper wires of negligible resistance to a power source. The temperature sensor is screwed onto the back of the sample-holder and thermalized over the copper-cylinder shown in Figure 4. The whole sample holder is covered with a thin copper plate, see Figure 5, in order to shield the resonator and the temperature sensor from direct radiation from the $40\,K$-shield.

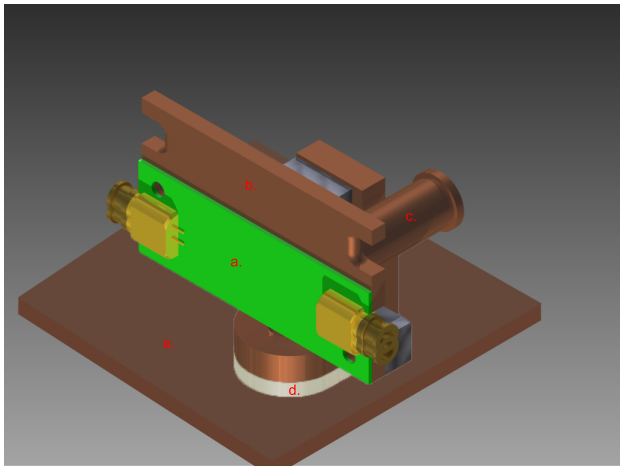

Figure 4: Front-side of the sample-holder: a. Chip, b. space for heating wire, c. thermalization for temperature sensor, d. FRP damper and e. 4 K-stage.

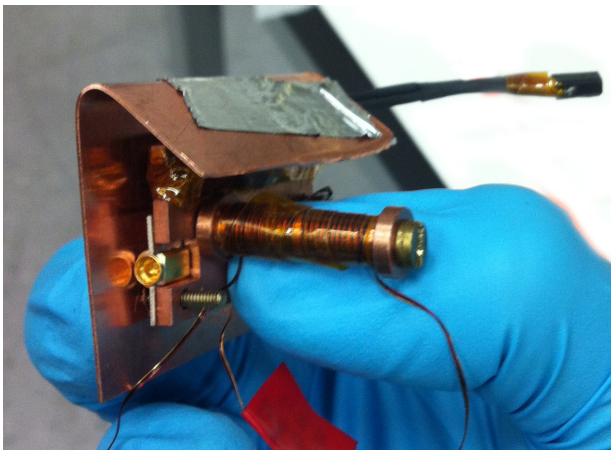

Figure 5: Sample-holder with heater and copper-shield.

3.4 Resonator

The waveguide on the chip consists out of the conducting material Niobium Titanium Nitride (NbTiN), with a resistance $\rho(T_c) = 9.36 \times 10^{-7}\,\Omega m$ and $T_c = 13.1\,K$ and the dielectric substrate used is sapphire with a dielectric constant $\epsilon_r = 10.7$ [2].

3.5 Signal Generator

For an active temperature control first the signal generator *33250A* from *Agilent* was used as a power source for the heater. Triggered by a 50 Hz signal, it was used to drive different waveforms on the heater to see what effect they have on the temperature fluctuations. It was possible to switch between a sine-wave, a square-signal, a triangular-signal or pulses directly. For each of the different waveforms, it was possible to set the frequency f in Hz, the high- and low-levels in volts and for the square signal a duty cycle in percent.

3.6 LabView Computer & DAQ Card

For an improved version of the temperature control a computer equipped with a *NI*[11] *PCI-6221 DAQ Card* connected to a *NI BNC-2110* shielded connector block was used. The DAQ card was controlled with a LabView program that was written for this purpose[12]. The Input of the DAQ card was connected to the analog output A of the LakeShore Model 340 temperature controller with the temperature sensor on the upper SH tunneled to the analog output A (Figure 6). The scale was set, such that $0 - 10\,V$ corresponds to a temperature scale of $0 - 10\,K$. Thus maximum resolution of the temperature was achieved. The systematic error of the LakeShore Model 340 temperature controller [10] is $1.25mK$ for the analog output.

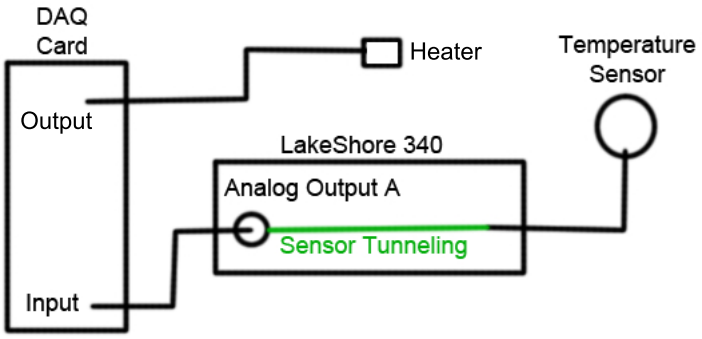

Figure 6: Temperature sensing setup.

The LabView program allows to make precise measurements of the temperature of the sample-holder with a time resolution of $20\,ms$[13]. The measurements can be saved into a ".dat" file with specified path and values separated with a tab. At the same time the LabView program allows to generate two voltage waveforms which will be added and given out on the output of the DAQ card. The two signals can chosen to be of square, sine or triangle step form and their frequency, amplitude and duty cycle can be set arbitrarily. The output of the DAQ card is connected to a current source[14], which is then connected to the heater on the sample-holder. In order to control the temperature, currents of at least $15\,mA$ are needed. Since the DAQ card has a maximum output current of $5\,mA$ the output signal needs to be amplified in order to reach a valid heating current. The generated signal will control the temperature of the sample-holder which can be manually adjusted by alternating the frequency and amplitude of the signals, so that the phase-shift between the temperature signal and the generated signal is exactly π.

[11] *National Instruments*

[12] For the full LabView program, see appendix B.

[13] The resolution is just this good if all other inputs from the same channel (A,B,C or D) are disabled. Otherwise the time resolution gets worse as described in chapter 3.2.

[14] Why this is needed see next paragraph. For further details see chapter 3.7.

3.7 Current Source

For the current source a simple circuit is used, that can be found in Appendix C. The circuit was alternated to suit the specifications needed for this experiment. The maximum load current is set to be $I_{load,max} = 300\,mA$ for a maximum input voltage of $V_{in,max} = 10\,V$. In order to reach this value the resistance denoted R_1 was changed to a value of $R_1 = 33\,\Omega$[15]. For the operational amplifier (OPA) an *OPA 227* was used. For the MOSFET denoted by Q_1 or $2N5459$ the *BF 245B* was inserted. The transistor Q_2 or $2N5192$ is integrated with a *BD 681G*.

The whole circuit was placed in a metal box with connectors for all the parts, and the transistor was screwed onto a heat pipe for cooling purposes.

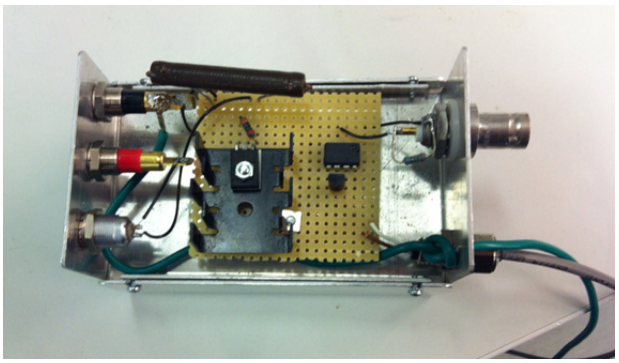

Figure 7: Current source with connectors.

The general principle of this circuit is that the OPA tries to maintain zero potential between its negative input port and the ground of the circuit. By doing so it applies a voltage to its output port that controls the MOSFET transistors, at a certain voltage the MOSFET "opens" and supplies a current which controls the NF-transistor. Once this current is high enough the NF-transistor amplifies the current to maintain the circuit "open". As soon as the circuit is "open", a current specified by the resistance R_1 can run through the load. Therefore the current through the load is controlled by the input voltage, following the formula $I_{load} = \frac{V_{in}}{R_1}$.

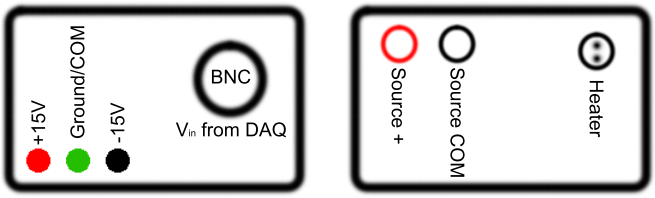

Figure 8: Current source connection legend.

For this circuit it is crucial, that the general ground is fixed to the zero potential of the OPA. Otherwise just the potential difference of 30 V between the +15 V and -15 V port of the OPA is defined and the circuit can accumulate charge and thus

[15]Since this resistance is heating up, a ceramic wrapped resistance was used.

increase or decrease its potential. Further the OPA needs the general ground as a reference point for the input-voltage, such that it is clear which potential it needs to try to bring into equilibrium. If the zero potential of the OPA is not fixed to the general ground the circuit loses its functionality and maximum current (300 mA) is always supplied!

3.8 Current Probe Amplifier

In order to measure the currents produced by the current source and the signal generator, a *Tektronix AM 503 Current Probe Amplifier* was used. The current probe was simply attached with its tongs to the wire of the heating circuit. Furthermore it was connected to a *LeCroy WaveRunner 6 Zi Oscilloscope* to save the resulting current signal. The current probe can be calibrated such that the voltage signal on the oscilloscope [V] is a one to one representation of the current running through the circuit [A]. Since the tongs of the current probe measure the magnetic field produced by the current running through the attached wires it is of great importance to separate the positive and negative wire and attach the tongs to one of them. If you would place the probe around both wires, the magnetic field cancels and it is not possible to measure a current.

The tongs have an iron core, which enhances the magnetic field produced by the current carrying wire. Inside the handle of the tongs, separating the two halfs of the iron core, a hall sond is placed to measure the magnetic field (Figure 9). Knowing the strength of the magnetic field, the current producing this field can be computed. Due to the small size of the iron core the current measurement is independent of the position of the wire within the tongs.

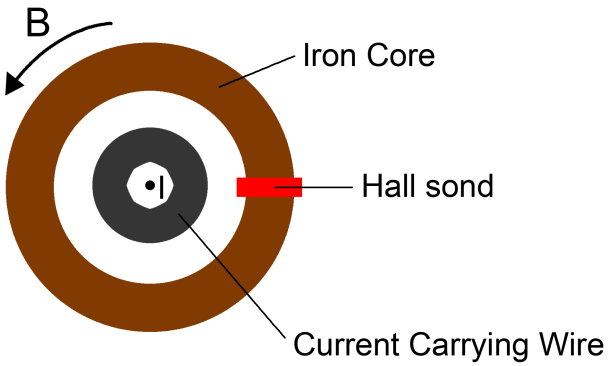

Figure 9: Schematics of the inside of the tongs of the current probe.

4 Measurements & Results

As described before an FRP damper was placed between the 4 K-Stage and the sample holder, reducing the temperature oscillations from initially 200 mK down to 68.5 mK. This FRP damper was kept in place throughout the course of the following measurements. Due to the weaker thermal conductivity of the FRP damper, the temperature of the sample-holder was increased, by 0.77 K.

In the following sections the measurements and results from the active temperature control are being presented. Since an active temperature control needs a source of heat (here heater) that is applied onto the sample-holder, the average temperature of the sample-holder is increased in addition to the 0.77 K from the FRP damper.

In order to get the best resolution in the temperature measurements, all the temperature sensors, besides the one on the sample-holder, were disabled in the control menu of the LakeShore 340. This allowed a readout-rate of $50\,Hz$, for the temperature sensor in question. For more than one signal per input channel[16], the readout-rate decreases by a factor of $(0.5)^{n-1}$, where $n \in \{1, 2, 3, 4\}$ is the number of measured sensors.

4.1 Temperature Control with PID-Controller

At first the inbuilt PID-Controller of the LakeShore Model 340 Temperature Controller was used for stabilization of the oscillations of the temperature on the sample-holder. Before the measurements were started the auto-tune feature of the PID-Controller was used to get a rough estimate of the range of values of the PID-gains. For the actual measurements the PID-Controller was tuned according to the Ziegler-Nichols method, see section 2.3. A comparison of the auto-tuned values with the ones obtained from the Ziegler-Nichols method can be found in Table 2. The values for the PID-gains, calculated with the PI-rule from Ziegler-Nichols, were relatively close to the ones from the auto-tune feature of the PID-Controller, see Table 2. Though it was observed, that the temperature fluctuations were reduced from 68.5 mK to 54.0 mK with the calculated values (measurement #5) instead of 55.0 mK with the auto-tuning (measurement #2).

The measurement sequence given in Table 2 was done with a $52\,\Omega$ constantan heater, installed on the sample-holder. Given the measured values for the peak-to-peak temperature fluctuations it is clear, that the PID-Controller was able to lower the fluctuations better at a higher setpoint temperature, see Figure 10.

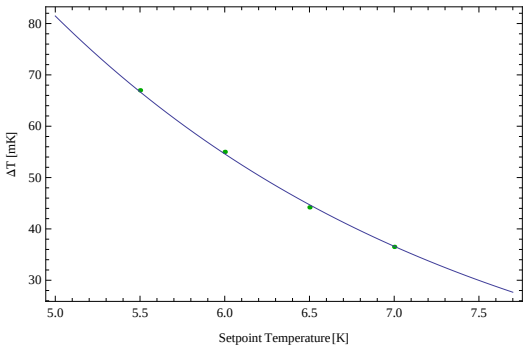

Figure 10: Setpoint temperature vs. peak-to-peak amplitude of the oscillations. The blue line just serves as a guide for the eye.

This is in accordance with the user's manual of the LakeShore 340 [10] which suggests the setpoint to be set at least $2 - 4\,K$ above base temperature of the pulse tube cooler for optimal PID-control. This is due to the fact, that for lower setpoint

[16] Input channels are A, B, C, D whereas C and D can have 4 input signals.

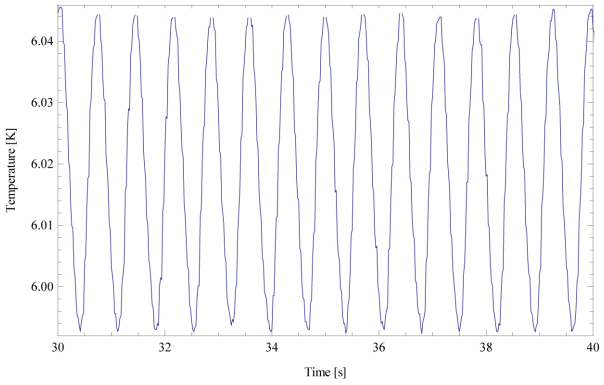

Figure 11: Measurement #6: Temperature fluctuations on the sample-holder.

temperatures the PID controller needs to overshoot much stronger than for higher temperatures. The system can not respond quickly enough to the high overshoot, due to its large respond time (1 s).

Even though the setpoint temperature needs to be set significantly higher than the base temperature, we still tried to accomplish good temperature control at a setpoint of $6\,K$, in order to stay in a temperature regime with good superconductivity features of the resonator. After the PID values for the $6\,K$ setpoint had been calculated with the Ziegler-Nichols method, an attempt was made to manually adjust the PID-gains, such that the temperature fluctuations were reduced. By trying different values around the ones calculated, it was possible to reduce the temperature fluctuations down to $\Delta T = 52.5\,mK$ from initially 68.5 mK, as shown in Figure 11.

In accordance with the suggested 2-4 K higher setpoint temperature, the best possible temperature control, with fluctuations of $\Delta K = 36.5\,mK$, was achieved at a setpoint of $T_S = 7.0\,K$ (2 K above base temperature of 5.1 K). The temperature fluctuations reduced further as the setpoint temperature increased. The tradeoff of having a higher, but very stable temperature on the sample-holder is not a very good option for the planned experiments to be done with this setup. Therefore the PID-Control solution is not ideal for this problem, since we want a sample temperature that is as close as possible to the base temperature of the pulse tube cooler. Furthermore, the option of raising the temperature of the sample to values higher then $13\,K$ ($T_c^{NbTiN} = 13.1\,K$) would be good to have, in order to study the resonance characteristics of the resonator at higher temperatures.

Measurement #	**Setpoint [K]**	**P**	**I**	**D**	ΔT **[mK]**
1 (AT)	5.5	10.0	152.4	0	67.0 ± 1.25
2 (AT)	6.0	12.5	145.0	0	55.0 ± 1.25
3 (AT)	6.5	12.5	145.0	0	44.2 ± 1.25
4 (AT)	7.0	15.6	191.3	0	36.5 ± 1.25
5 (ZN)	6.0	11.7	139.5	0	54.0 ± 1.25
6 (MT)	6.0	12.0	142.2	0	52.5 ± 1.25

Table 2: Measurements with active control by PID Controller. Setpoint temperature, PID gain settings and resulting peak-to-peak temperature fluctuation. AT=Autotune, ZN=Ziegler-Nichols Method, MT=Manually tuned.

4.2 Determining the Oscillation Frequency

The temperature fluctuations on the sample-holder were observed to have a very distinct frequency and were sinusoidal shaped. Therefore the idea for the following measurements was to counteract the oscillations with a signal of the same frequency that is shifted by a phase of π. In order to find the frequency of the fluctuations, the temperature oscillations at the sample-holder with the FRP dampers were recorded for 4 minutes and then fouriertransformed to find the characteristic frequency. In the fourier-transform, the sample rate is limiting the highest resolvable frequency and the sample length limits the smallest resolvable frequency. Specifically for the discrete fourier transform it is important, that the beginning and the end of the data match in a periodic fashion. The spectrum, see Figure 12, shows a very distinct peak at $f_0 = 1.411775\,\mathrm{Hz}$ and its corresponding higher harmonics.

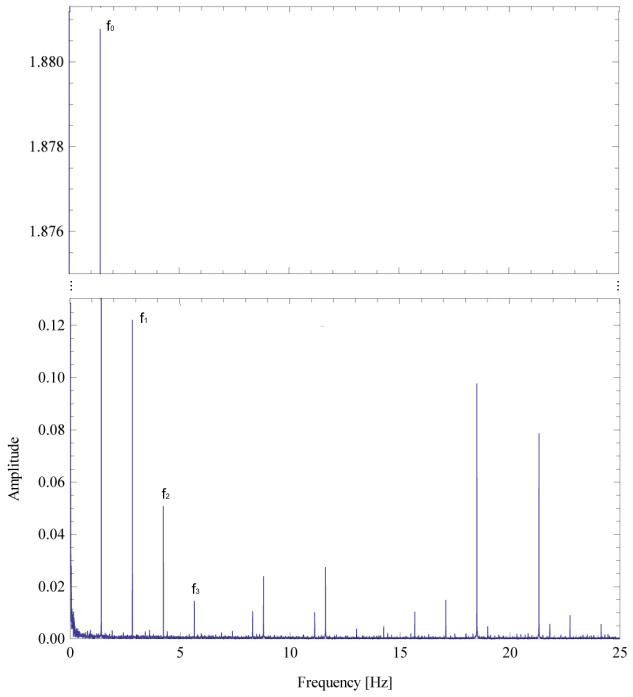

Figure 12: Spectrum of the temperature oscillations on the sample-holder. A measurement of 4 minutes was fourier-transformed. The main frequency at $\backsimeq 1.41\,\mathrm{Hz}$ is clearly observable.

For the same purpose a longtime measurement, over 8 hours, of the temperature oscillations was done, in order to see whether a sine wave with this frequency might lose its phase after a while, due to slight changes in the fluctuation frequency. The longtime measurement was used to fit a sine wave through the data points using the "FindFit" function of Mathematica, see Appendix A.2. The fitting algorithm calculated the frequency of the temperature oscillations to be

$$f_0 = 1.41178\,\mathrm{Hz}.$$

Plotting a sine wave with this frequency onto the longtime measurement showed, that the phase was kept stable over the measured time, see Figure 13.

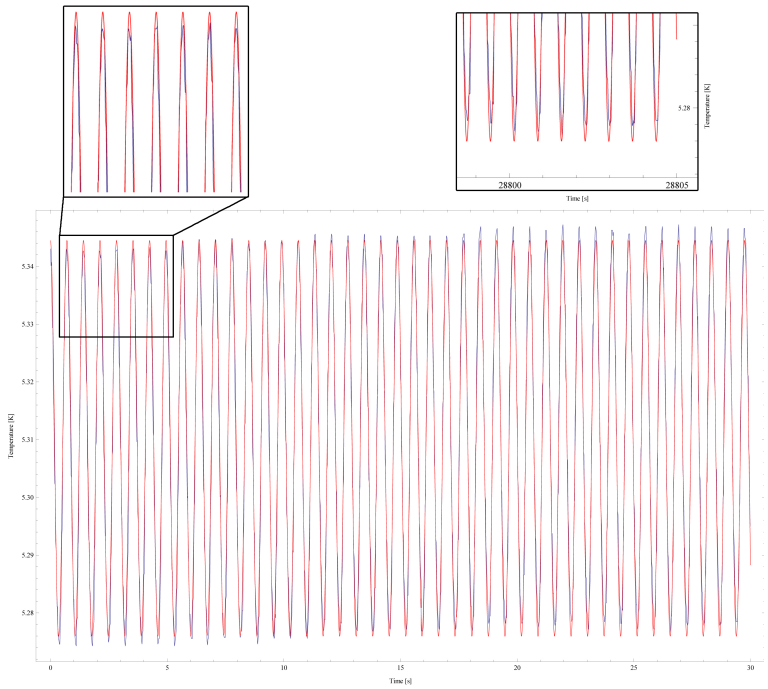

Figure 13: Plot of sine wave (red) with frequency $f_0 = 1.41178$ Hz over a part of the longtime measurement (blue). The inset on the top right shows the longtime measurement with the sine wave after 8 hours. It is obvious that the phase between the oscillations and the sine wave is not lost at this point.

Before starting the actual measurements of the temperature stabilization, the response time of the system was measured. This was done to see whether the system responds fast enough to an applied heating signal. The response time of the system turned out to be $t_R = 1\,s$, see Figure 14, which is fast enough for controlling the temperature.

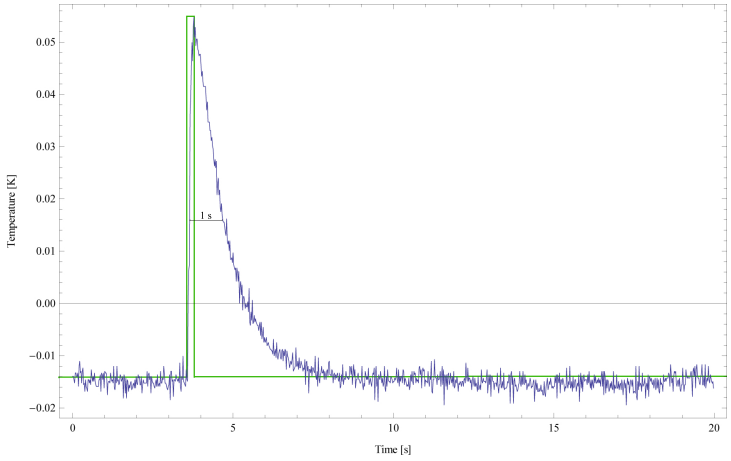

Figure 14: Response (blue) of the system (sample-holder with heater) to a 100 ms long pulse with amplitude 1 V (green). The response was obtained by measuring the temperature with and without the pulse and subtracting the resulting data.

4.3 Temperature Control with Frequency Generator

In the following measurement sequence a frequency generator from Agilent, see section 3.5, was used to generate a heating signal with the heater on the sample-holder. An attempt of reducing the fluctuations was done with different signal types[17] to find the one with the best result. The average temperature has been kept as low as possible and usually corresponded to a value around $T_{averge} = 5.6\,K$. The lower level of the signal was fixed to zero volts and the higher-level adjusted such that the temperature fluctuations were at their minimum. The phase of the signal was set by raising and lowering the frequency, until the generated signal had exactly a phase of π corresponding to the temperature fluctuations. Then the frequency of the signal was set to the calculated value of $f_0 = 1.41178$ Hz.

The best results were achieved by applying this procedure with a non-symmetric square signal. By tuning the duty cycle of the square signal, see Table 3, it was possible to reduce the temperature fluctuations to a value of $\Delta T = 8 \pm 1.25\,mK$,see Figure 15, from initially $200\,mK$. Tuning the duty cycle of the square signal, makes it possible to take the response time of the system into account, which is not possible with the other waveforms.

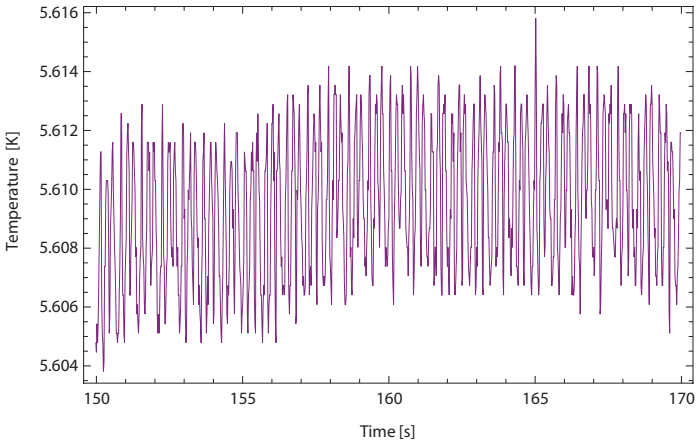

Figure 15: Measurement #4: Temperature fluctuations of $\Delta T = 8 \pm 1.25\,mK$ of the sample-holder, using a square signal.

The measurements from the other signals, see Appendix D.1, suggest, that now the frequency of the reduced temperature oscillations have a higher frequency in comparison to the once without active control. The frequency is three times as big, as can be seen in Figure 16 & 17. For the sake of easier control and due to the idea of applying a second signal with a higher frequency to reduce the fluctuations even more, the signal generation was implemented in LabView. This is the next step in this thesis and is presented in the following section 4.4.

[17] sine-, square- and triangle-signal

Measure-ment #	**Signal Type**	**Hi-Lev. [mV]**	**Low-Lev. [mV]**	**d. cyc. [%] sym. [%]**	ΔT **[mK]**
1	Sine	903	0	-	13.0 ± 1.25
2	Square	850	0	50	9.35 ± 1.25
3	Triangle	1100	0	30	13.0 ± 1.25
4	Square	857	0	55	8.0 ± 1.25

Table 3: Measurement sequence with signal generator. Signal-type, signal-settings and resulting peak-to-peak temperature fluctuation.

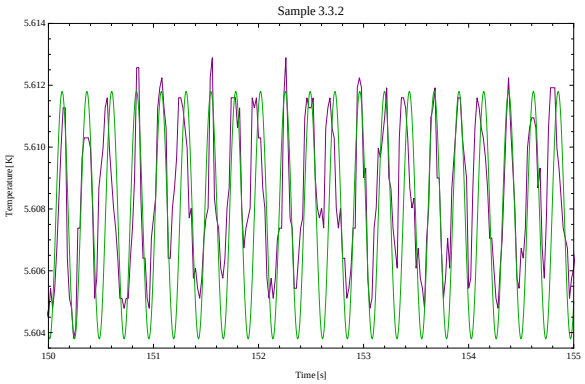

Figure 16: Temperature oscillations from measurement #4 (purple) with fitted sine wave (green) with three times the original frequency f_0.

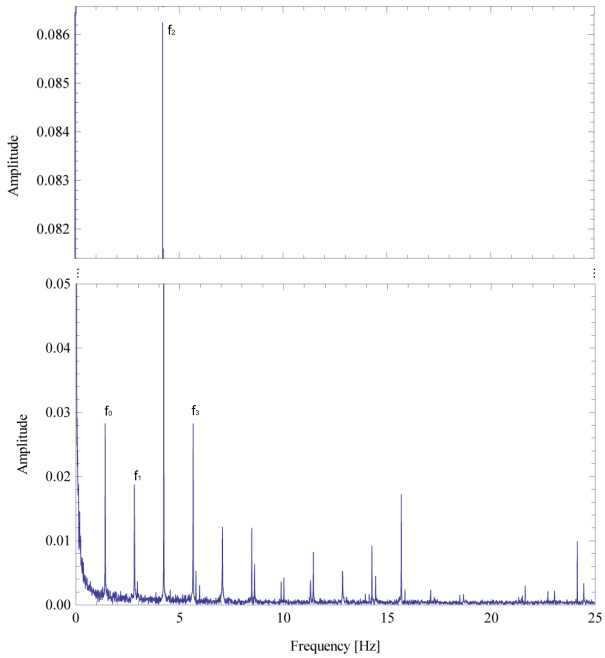

Figure 17: Spectrum of the temperature oscillations from measurement #4. The distinct peak at $f_2 \simeq 4.235$ Hz shows, that the dominating frequency in the reduced temperature oscillations is the second harmonic of the initial frequency f_0.

4.4 Temperature Control with LabView & DAQ Card

To enhance the temperature control of the sample-holder a LabView program connected to a DAQ card (NI PCI-6221 DAQ Card*)* was used, setup see section 3.6 and 3.7. As described in chapter 4.3 the phase of the signal can be set by changing the frequency. Due to the encountered problems with the pulse tube cooler, described in chapter 3.1, it was not possible to conduct temperature control measurements with the LabView/DAQ setup within the time frame of this semester-thesis.

4.4.1 Current Characteristics and Proof of Equality

In order to show that the signal generation with the LabView program, through the connected DAQ card and current source, is able to provide the same temperature control as the signal generator does, their current characteristics were measured and compared. Furthermore it was shown that the LabView program can generate the same current signal as the signal generator. For the current measurements the *Tektronix AM 503 Current Probe Amplifier*, see section 3.8, and a dummy heater with a resistance of $R = 100\,\Omega$ were used.

The current signal of the two setups was measured for different input voltages and plotted in Figure 18. As expected, both of the setups show a linear voltage-current characteristic but differ in their slope. Using the "Fit-Function" in Mathematica a linear model was fitted through the measured data, see Appendix A.3, in order to get the following voltage-current relation Equation (7) is for the signal generator and Equation (8) for the LabView/DAQ setup.

$$I_{Gen} = 0.0742201 + 12.6499 \cdot V \ [mA] \tag{7}$$

$$I_{DAQ} = 2.03993 + 26.1058 \cdot V \ [mA] \tag{8}$$

Since the voltage-current relation is $I = \frac{U}{R}$, the inverse of the slope should return the resistance of the circuit.

$$R_{Gen} = 79.05\,\Omega \tag{9}$$

$$R_{DAQ} = 38.31\,\Omega \tag{10}$$

The resistance from the model for the signal generator, Equation (9), is smaller than the resistance used as a dummy heater. This is due to a resistance within the signal generator, which is connected in parallel to prohibit a shortage in the electronics of the signal generator. A measurement proofed that the missing resistance is equivalent to $R = 400\,\Omega$. Calculating the replacement resistance,

$$R_{rep} = \left[\frac{1}{400} + \frac{1}{100}\right]^{-1} = 80\,\Omega,$$

which is the slope of the voltage-current curve of the signal generator. Therefore it is obvious that the replacement resistance is the resistance that characterizes the current of the signal generator to a fixed voltage. For the model of the LabView setup the resistance is exactly the resistance R_1 that determines the current through the load within the current source, see section 3.7. Therefore for this setup it does not matter what the resistance of the heater is, it will always follow the same (Figure

18 orange line) voltage-current characteristic. The offset of the current-model for the signal generator negligibly small (∼0.074 mA. Whereas the offset of the model for the DAQ setup is due to a small leakage current at zero input voltage (∼2.04 mA), which was also measured.

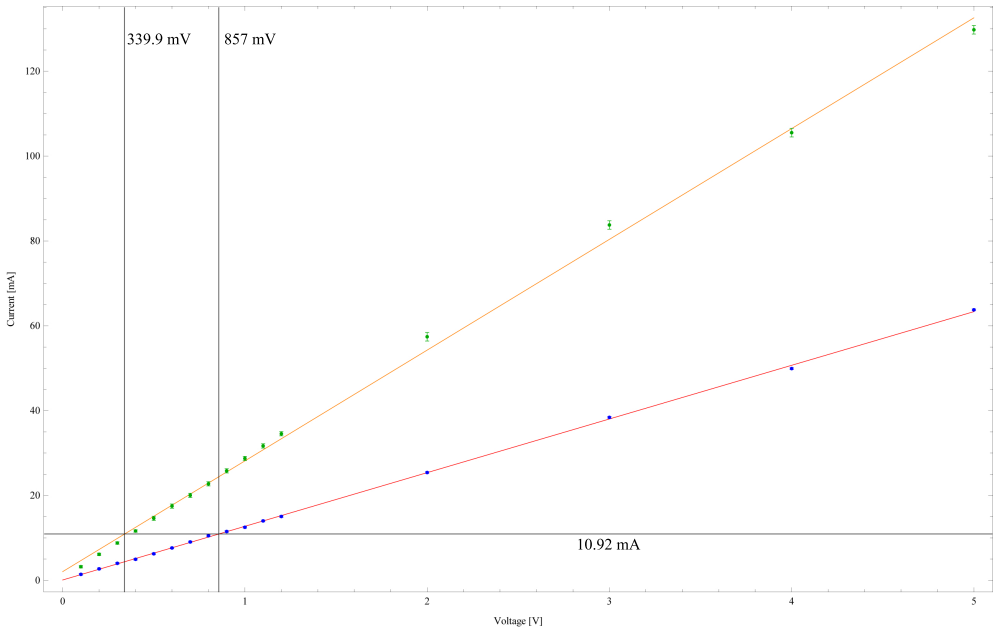

Figure 18: Voltage-Current curve of the signal generator (blue dots and fitted red line) and DAQ card with the current source connected (green dots and fitted orange line). For the DAQ setup the input voltage was alternated within LabView and the current source was connected to a current supply at with constant voltage of 20 V. For the signal generator just the High-Level was alternated and the Low-Level was held constant at 0 V.

In order for the LabView setup to have the same heating characteristics as the signal generator, their currents have to be equal and their signals need to be of the same shape. With the calculated models for the voltage-current characteristic we were able to find the voltage at which the LabView setup produces the same current as the signal generator at optimal temperature control, as described in chapter 4.3 (High-Level: 0.857 V, Low-Level: 0 V). Therefore to reach the same temperature control as with the signal generator, we have to set an input voltage (i.e. amplitude) in the LabView program of 339.973 mV, see Figure 18. Furthermore Figure 19 shows, that the signal forms of the two devices are equal to first order in time and are just shifted in amplitude due to their difference in slope in the voltage-current curve.

Given the above analysis the temperature control setup implemented on LabView will produce similar results to the one with the signal generator.

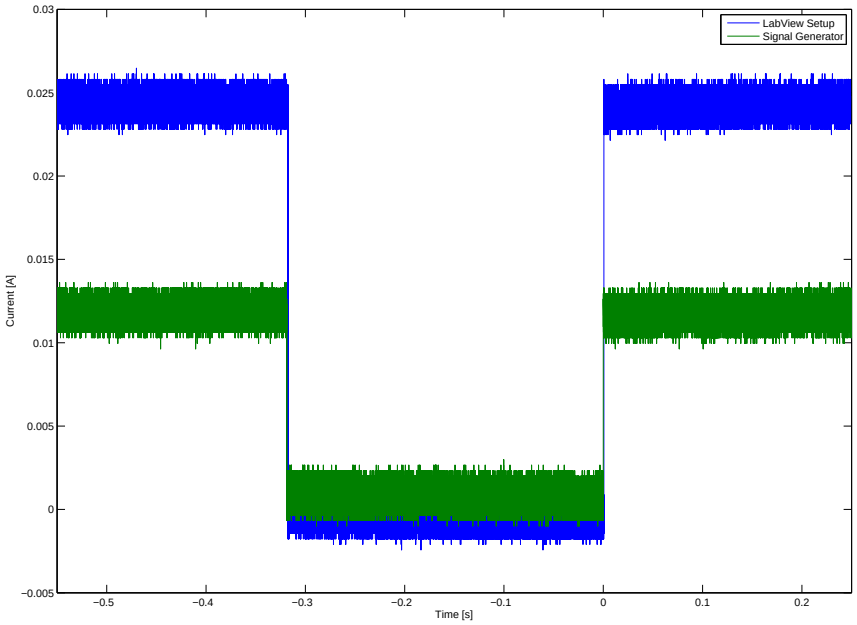

Figure 19: Current signal of the signal generator (green) and the LabView setup (blue) at a voltage of 800 mV.

5 Summary

The presented measurements showed, that the temperature fluctuations on the sample-holder can be reduced by using a combination of active and passive temperature control mechanisms. It became clear that the inbuilt PID-controller of the LakeShore 340 is not good enough to serve the needed requirements. Therefore a double signal generation with LabView was implemented, that will reduce the temperature fluctuations to about 4% of its initial value of 200 mK at an increase of base temperature of 0.77 K at 4.6 K. The same temperature control at $T_{Base} = 2.9\,K$ should result in a similar increased base temperature.

6 Outlook

The implemented temperature control can be further enhanced by programming a module that automatically sets the required phase onto the generated signals. Further it might be good to implement a PID control mechanism in LabView that controls the temperature totally automatic. The PID control feature in LabView might be much faster than the one from the LakeShore 340, it also might be able to control the temperature at a much lower setpoint than the LakeShore 340.

A Mathematica Codes

A.1 Code for the Calculation of the Power-Spectrum

```
tempdata =
  Import[
   "R:\\USERS\\Matthias Mergenthaler\\Temperature
     Measurements\\TempLog_SH2_Sample_1_2012-06-18.dat"];

Data = ({{#[[1]], #[[2]]}} & /@ tempdata[[1 ;; 1500, {1, 2}]])^T;

vals = ({#[[2]]} & /@ tempdata[[1 ;; 1500, {1, 2}]])^T;

ft = Abs[Fourier[vals]];

xvalues = Table[(x - 1) / 30, {x, 1, 1500}];

Liste = Table[{xvalues[[i]], ft[[1]][[i]]}, {i, 1, 1500}];

ListPlot[Data, PlotRange → All, Joined → True, Frame → True,
 FrameLabel → {"Time [s]", "Temperature [K]"}]
ListPlot[Data, PlotRange → {{1, 5}, {5.27, 5.35}}, Joined → True, Frame → True,
 FrameLabel → {"Time [s]", "Temperature [K]"}]
ListLinePlot[Liste, Joined → True, PlotRange → {{0, 25}, {0, 0.55}}, Frame → True,
 FrameLabel → {"Frequency [Hz]", "Amplitude"}]
ListLinePlot[Liste, Joined → True, PlotRange → {{0, 25}, {0, 0.04}}, Frame → True,
 FrameLabel → {"Frequency [Hz]", "Amplitude"}]
ListLinePlot[Liste, Joined → True, PlotRange → {{1.395, 1.41}, {.4, .535}}, Frame → True,
 FrameLabel → {"Frequency [Hz]", "Amplitude"}]
```

A.2 Code for FindFit

```
tempdata =
  Import[
   "R:\\USERS\\Matthias Mergenthaler\\Temperature
     Measurements\\TempLog_SH2_Sample_1_2012-06-18.dat"];


Data = ({{#[[1]], #[[2]]}} & /@ tempdata[[1 ;; 1500, {1, 2}]])^T;

Data[[1]];

fitparam = FindFit[Data[[1]], A * Sin[2 π f t + b] + c, {{A, 0.2}, {b, π / 2}, {f, 1.4}, {c, 5.3}}, t]

{A → 0.0342727, b → 1.6223, f → 1.41174, c → 5.31025}
```

A.3 Code for Voltage-Current Model

```
Needs["PlotLegends`"]

data1 = {{0.1, 1.4}, {0.2, 2.7}, {0.3, 4.0}, {0.4, 4.95}, {0.5, 6.25},
   {0.6, 7.625}, {0.7, 9.04}, {0.8, 10.5}, {0.9, 11.5}, {1, 12.5},
   {1.1, 14.0}, {1.2, 15.04}, {2, 25.4}, {3, 38.4}, {4, 49.9}, {5, 63.75}};
data2 = {{0.1, 3.2}, {0.2, 6.125}, {0.3, 8.79}, {0.4, 11.625},
   {0.5, 14.615}, {0.6, 17.495}, {0.7, 20.03}, {0.8, 22.74},
   {0.9, 25.795}, {1, 28.715}, {1.1, 31.675}, {1.2, 34.54}, {2, 57.4},
   {3, 83.75}, {4, 105.5}, {5, 129.75}};

Plot1 = ListPlot[{data1, data2}, PlotStyle -> {Blue, Darker[Green]},
   Frame → True, FrameLabel → {"Voltage [V]", "Current [mA]"}];

agi[x_] = Fit[data1, {1, x}, x]
daq[x_] = Fit[data2, {1, x}, x]

0.0742201 + 12.6499 x

2.03993 + 26.1058 x

Plot2 = Plot[{agi[x], daq[x]}, {x, 0, 5}, PlotStyle -> {Red, Orange},
   Frame → True, FrameLabel → {"Voltage [V]", "Current [mA]"}];

Show[Plot1, Plot2]
```

B LabView Program

B.1 LabView Front End

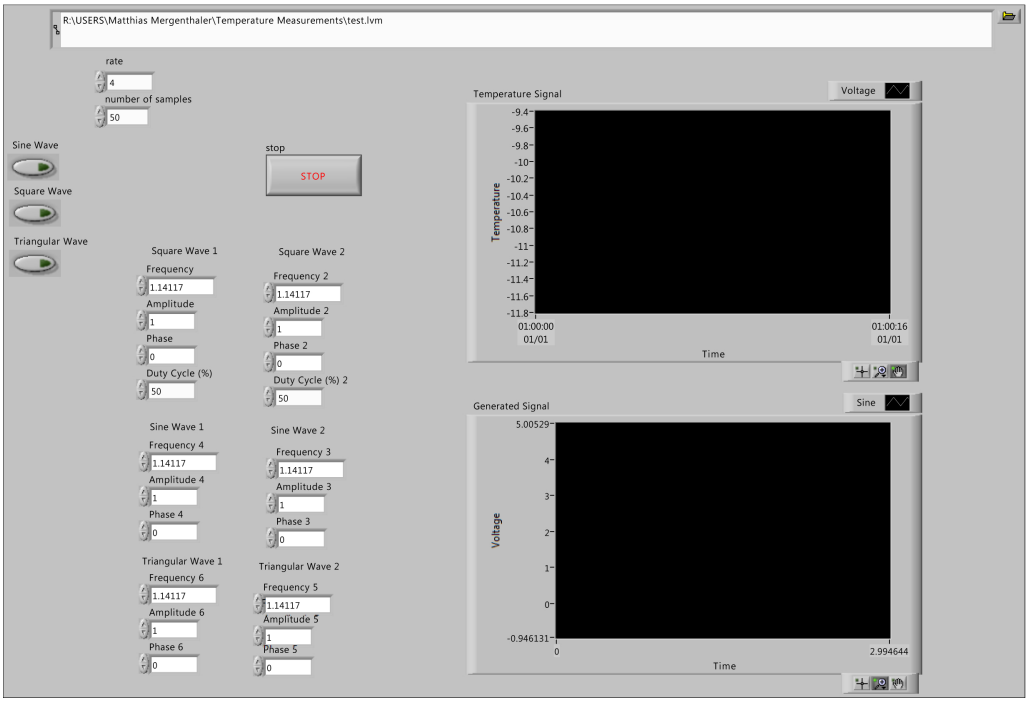

B.2 LabView Back End

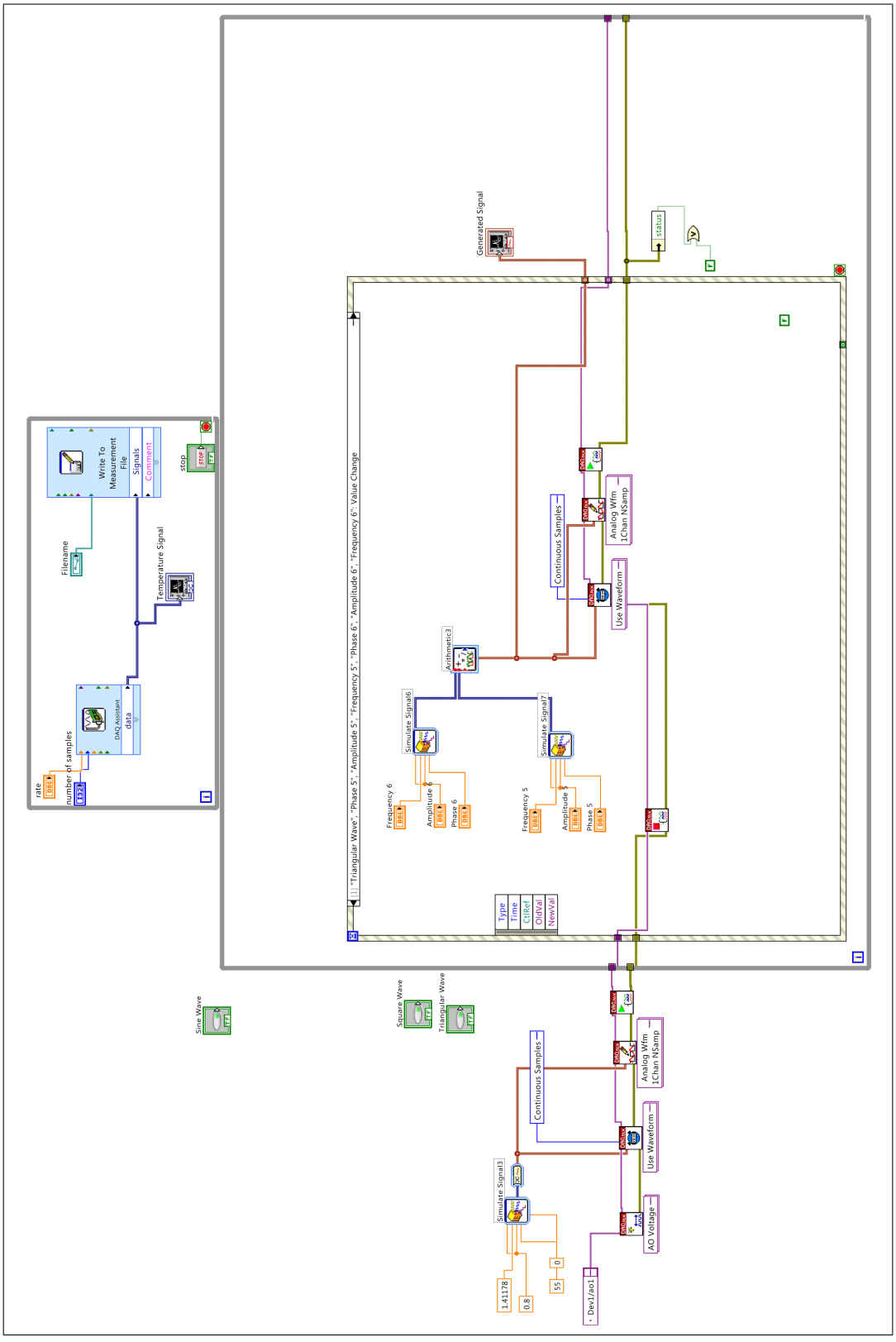

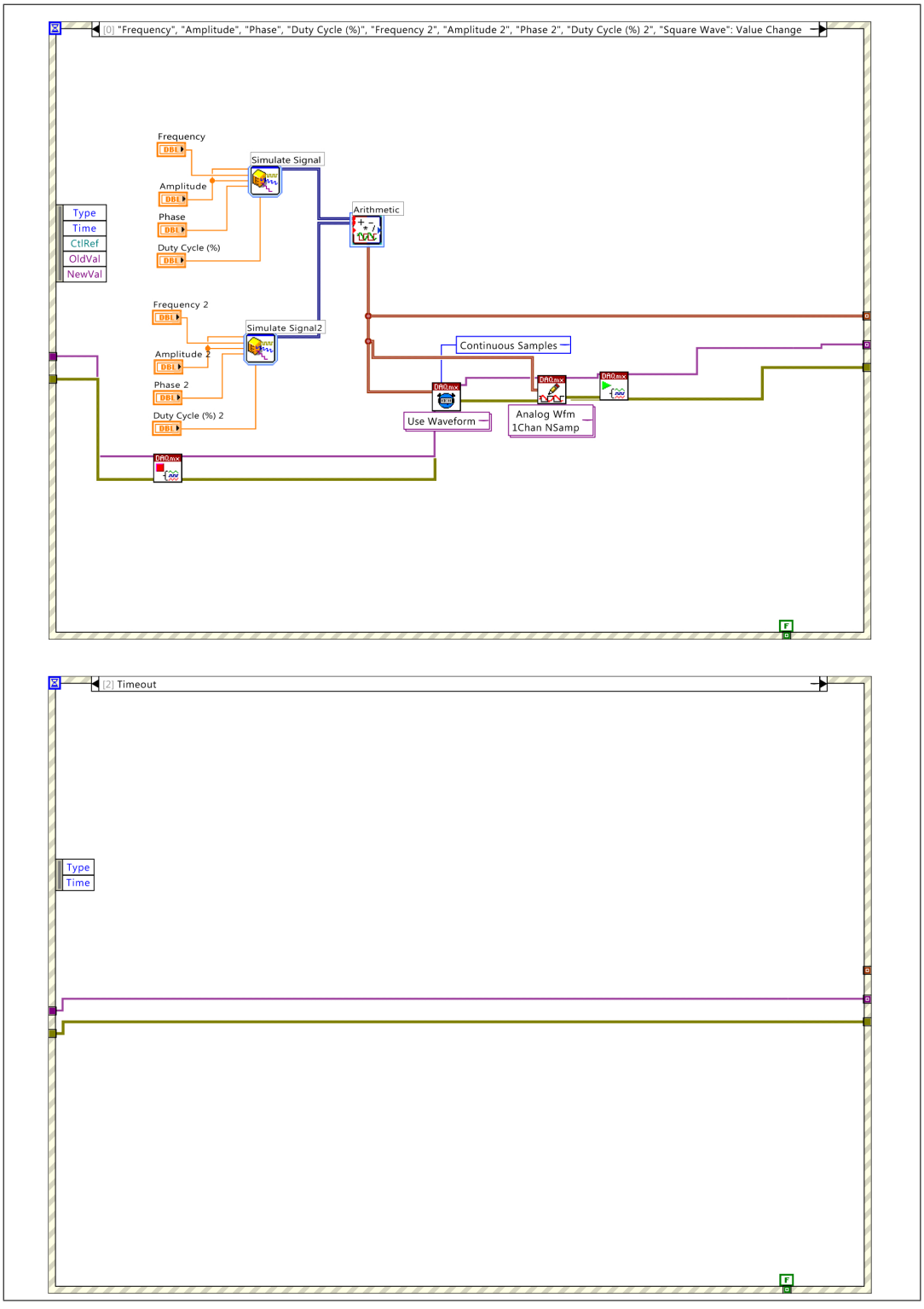
[0] "Frequency", "Amplitude", "Phase", "Duty Cycle (%)", "Frequency 2", "Amplitude 2", "Phase 2", "Duty Cycle (%) 2", "Square Wave": Value Change
Frequency
Amplitude
Phase
Duty Cycle (%)
Simulate Signal
Type
Time
CtlRef
OldVal
NewVal
Arithmetic
Frequency 2
Amplitude 2
Phase 2
Duty Cycle (%) 2
Simulate Signal2
Continuous Samples
Use Waveform
Analog Wfm
1Chan NSamp
[2] Timeout
Type
Time

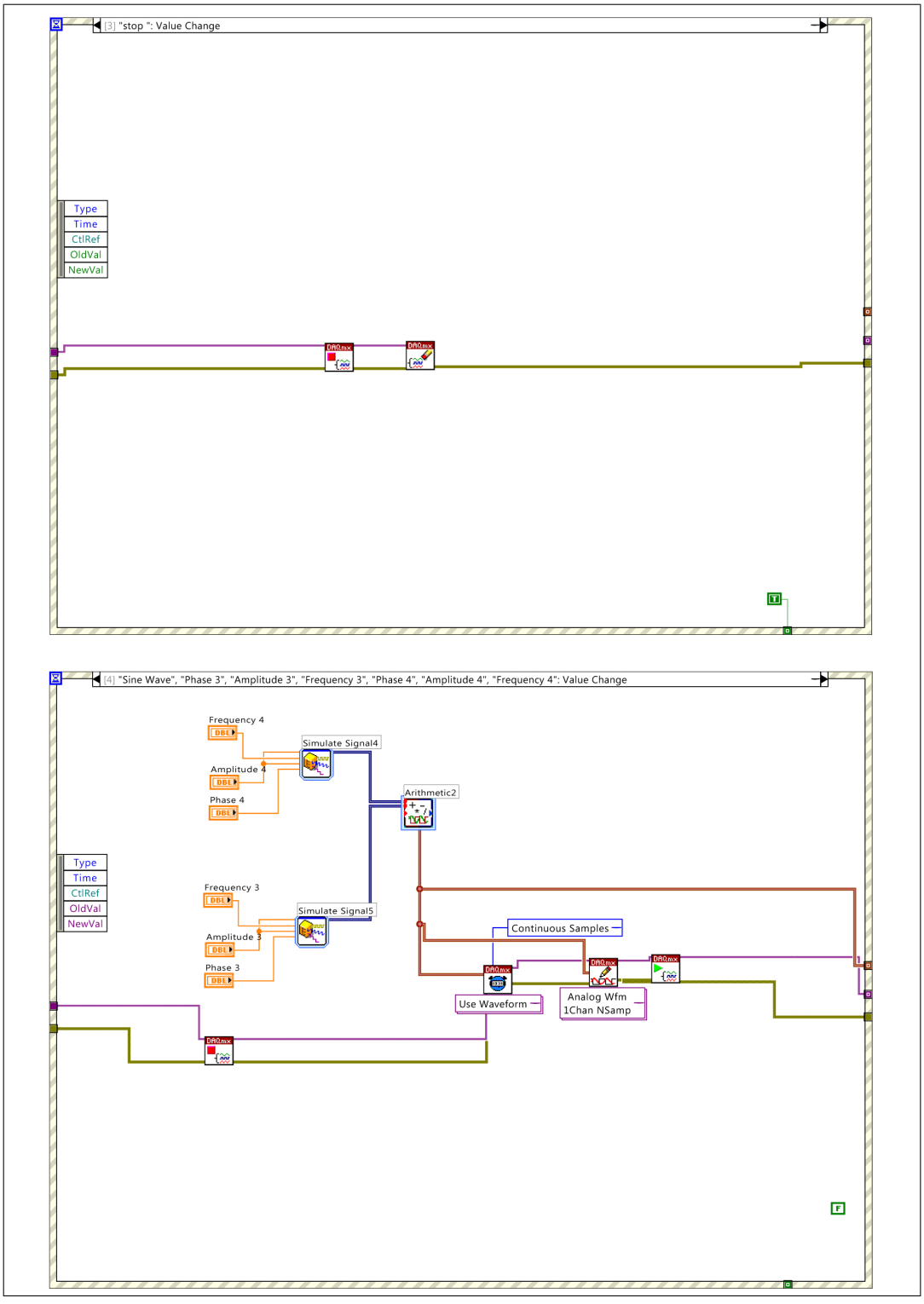
[3] "stop ": Value Change
Type
Time
CtlRef
OldVal
NewVal
[4] "Sine Wave", "Phase 3", "Amplitude 3", "Frequency 3", "Phase 4", "Amplitude 4", "Frequency 4": Value Change
Frequency 4
Simulate Signal4
Amplitude 4
Phase 4
Arithmetic2
Frequency 3
Simulate Signal5
Amplitude 3
Phase 3
Continuous Samples
Use Waveform
Analog Wfm
1Chan NSamp

C Circuit Diagram For Current Amplifier

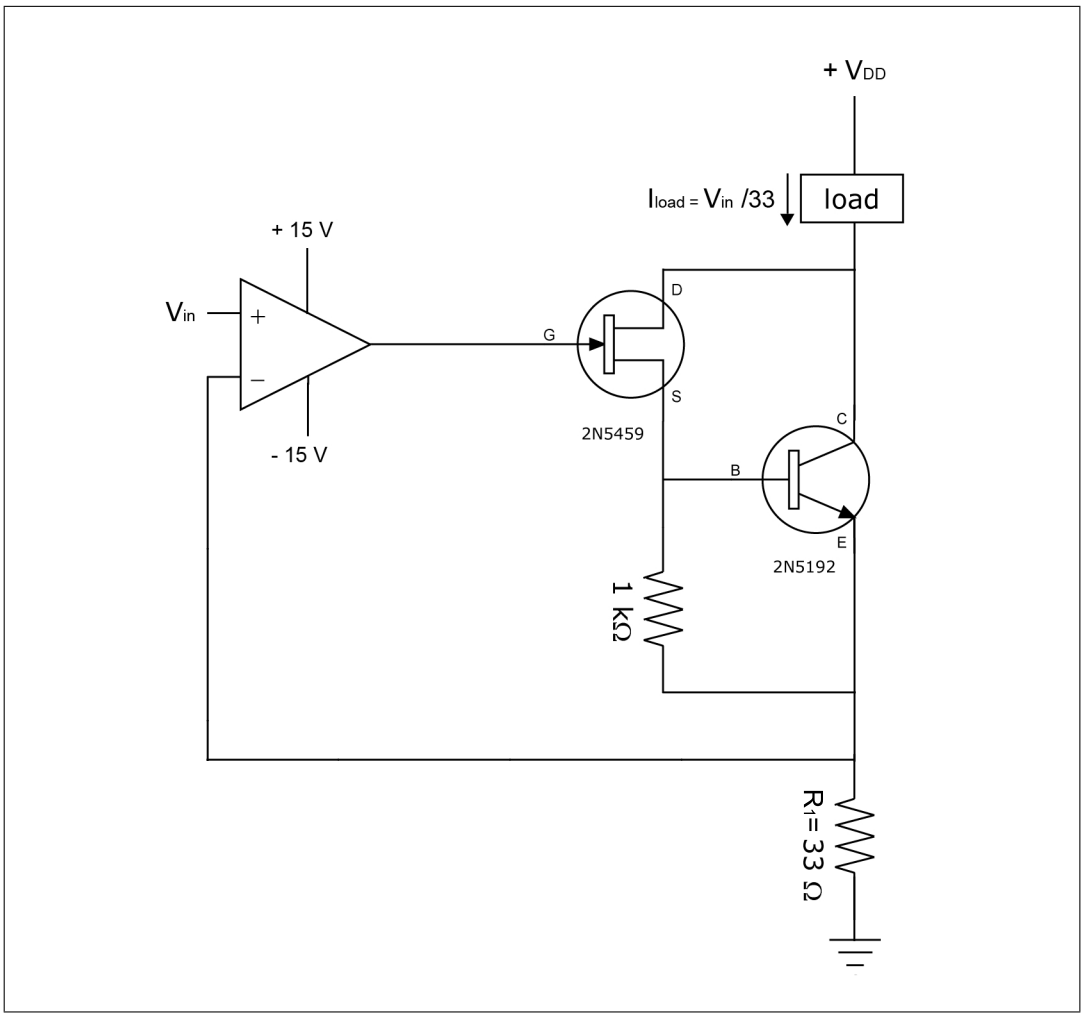

D Additional Graphs

D.1 Temperature Oscillations with Signal Generator

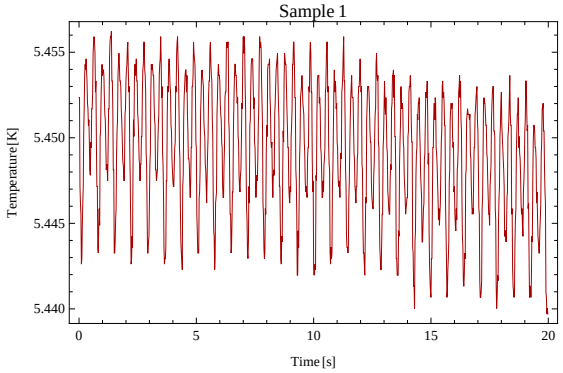

Figure 20: Sample #1: Temperature oscillations on sample-holder with a sine wave as heating signal.

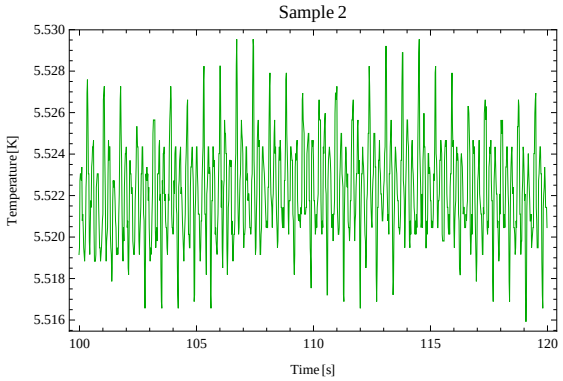

Figure 21: Sample #2: Temperature oscillations on sample-holder with a square signal as heating signal.

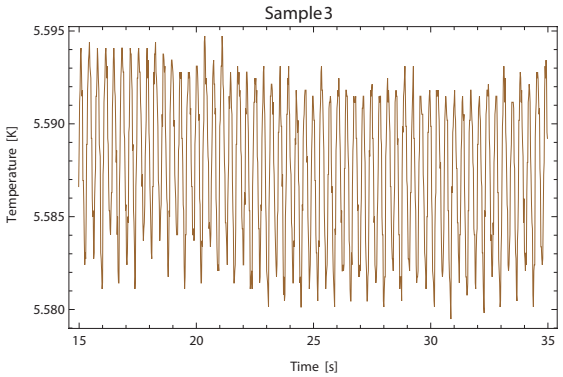

Figure 22: Sample #3: Temperature oscillations on sample-holder with a triangular signal as heating signal.

References

[1] Andreas Wallraff. Hybrid cavity quantum electrodynamics with atoms and circuits. 2008.

[2] Dominik Waldburger. Temperature dependent measurements of undercoupled coplanar NbTiN-resonators. Semester Thesis, ETH Zurich, 2012.

[3] Daiki Nakamura, Yasuhiro Hasegawa, Masayuki Murata, Hiroya Yamamoto, Fumiaki Tsunemi, and Takashi Komine. Reduction of temperature fluctuation within low temperature region using a cryocooler. *Review of Scientific Instruments*, 82(4):044903, 2011.

[4] Yasuhiro Hasegawa, Daiki Nakamura, Masayuki Murata, Hiroya Yamamoto, and Takashi Komine. High-precision temperature control and stabilization using a cryocooler. *Review of Scientific Instruments*, 81(9):094901, 2010.

[5] Inc. Boedeker Plastics. Boedeker plastics: Durostone frp fiberglass reinforced plastic solder pallet materials specifications. `http://www.boedeker.com/durost_p.htm`, 2012. [Online; accessed 15-July-2012].

[6] James Bennett, Ajay Bhasin, Jamila Grant, and Wen Chung Lim. Pid tuning classical. `https://controls.engin.umich.edu/wiki/index.php/PIDTuningClassical`, 2007. [Online; accessed 20-July-2012].

[7] Silvio Marx. Realization of temperature and vibration measurement systems for hybrid cavity QED experiments. Master's thesis, ETH Zurich, December 2010.

[8] S. D. Hogan, J. A. Agner, F. Merkt, T. Thiele, S. Filipp, and A. Wallraff. Driving rydberg-rydberg transitions from a coplanar microwave waveguide. *Phys. Rev. Lett.*, 108:063004, Feb 2012.

[9] Ray Radebaugh. Pulse tube cryocoolers for cooling infrared sensors. *Proc. SPIE 4130, Infrared Technology and Applications XXVI*, pages 363–379, December 2000.

[10] Inc. Lake Shore Cryotronics. User's Manual Model 340 Temperature Controller, March 2004.